Korean J. Chem. Eng., **16**(6), 709-720 (1999)

FEATURED REVIEW

Classification and Characterization of Hydrodynamic and Transport Behaviors of Three-Phase Reactors

Atsushi Tsutsumi†, Wei Chen and Yong-Han Kim*

Department of Chemical System Engineering, The University of Tokyo,
7-3-1 Hongo, Bunkyo-ku, Tokyo 113-8656, Japan
*Department of Chemical Engineering, Pukyong National University,
San 100, Yongdang-dong, Nam-Gu, Pusan 608-739, Korea

Abstract—According to axial profile of solid concentration, the cocurrent upward three-phase reactors with liquid as continuous phase can be classified into three types: (a) gas-sparged slurry reactors, (b) three-phase bubble columns, and (c) three-phase fluidized beds. Comparative study shows that the gas hold up, bubble characteristics and mass transfer are significantly dependent on the type of three-phase reactors. Three types of reactors exhibit the different hydrodynamic and transport behaviors with particle size, solid concentration and gas holdup. The structural analysis of the axial solid distribution indicates the bubble and bubble wake dynamics are the key factors to the hydrodynamic and transport behaviors of three-phase reactors.

Key words: Three-phase Reactors, Classification and Characterization, Hydrodynamic and Transport Behaviors

INTRODUCTION

The concept of 'three-phase reactor' includes all the reactors where gas, liquid and solid three phases exist simultaneously in contact with other phases. Such reactors can present various features of hydrodynamic behaviors depending on the type of discrete phases and flow direction of each phase. Based on the contacting mode of gas, liquid and solid phases, Fan [1989] proposed a classification of three-phase reactors which includes all kinds of three-phase reactors. Among these diversities, we will consider only the gas-liquid-solid system where gas and solid phases are dispersed in a continuous liquid phase (mode E-I-a and E-III-a in Fan's classification). Such types of three-phase reactors are by far the most commonly encountered industrial applications. In this paper, the term 'three-phase reactor(s)' represents for the column-typed three-phase reactors in which the gas and liquid flow cocurrently upward and the solid particles are fluidized by gas and/or liquid flows.

Despite their wide use in various industrial processes, it is well known that there is no sufficient knowledge of reactor design because of a large number of variables which are able to influence the performance of three phase reactors. In addition, individual research work in the literature usually put their focus on one aspect of the characteristics of the reactors. The systematic and comprehensive research work is scarce. This leads to the barrier of understanding the hydrodynamic and transport mechanisms of three-phase reactors.

The present paper describes the classification method of three-phase reactors based on the axial solid distribution profiles, and characterizes the hydrodynamic and transport properties of each type of three-phase reactors.

†To whom correspondence should be addressed.
E-mail: tsutsumi@chemsys.t.u-tokyo.ac.jp

CLASSIFICATION OF THREE PHASE REACTORS

In general, many types of three-phase reactors are divided into two categories according to the size of particles and the force causing the solid suspension.

Østergaard [1968] pointed out early that the bubble column slurry reactor can be distinguished from the usual fluidized bed where solid particles are fluidized by the upward liquid flow while the gaseous phases moves as discrete bubbles through the liquid-fluidized bed. Deckwer and Schumpe [1984] also proposed the similar classification method.

Epstein [1981] stated that three-phase bubble fluidization is distinguishable from bubble column slurry operation only in its use of large and/or heavy particles, which are not subject to the hydraulic transport characteristics of slurry operation when the liquid is moving.

Muroyama and Fan [1985] distinguished the three-phase fluidized-bed reactor form the gas-sparged slurry reactor according to particle size and solid concentration. In the gas-sparged slurry reactor, the size of the solid particle is usually less than 100 μm in diameter, the volumetric fraction of the solids is less than 0.1, and the particles are maintained in a suspended state by bubble agitation. In the three-phase fluidized bed, the particle size is relatively large, normally greater than 200 μm, and the volumetric fraction of the solid particles varies from 0.6 (packed state) to 0.2 (close to the dilute transport state). The particles are supported by the liquid phase and/or the gas phase.

Pandit and Joshi [1986] stated that the three-phase sparged reactors should be called gas-liquid-solid fluidized bed or slurry reactors, respectively, corresponding to batch-wise or continuous mode of operation for solid particles. They further divided the behavior of three-phase reactors in to four regions according to the effects of particle size and solid concentration on bubble diameter.

In spite of considerable discrepancy among the above classi-

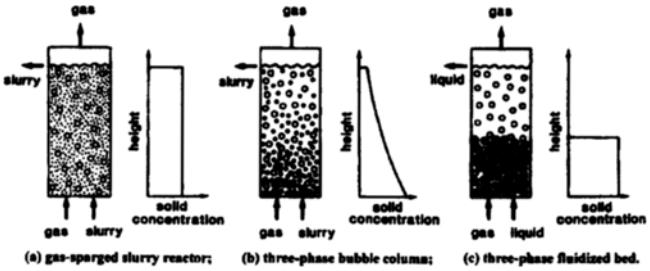

Fig. 1. Three types of three-phase reactors.
(a) gas-sparged slurry reactor, (b) three-phase bubble column, (c) three-phase fluidized bed.

fication methods, it can be recognized that there is general agreement among those papers that larger and/or heavier particles are used in three-phase fluidized bed than in slurry bubble column reactors. In the case of very large and/or heavy particles the bed consists of the upper dilute region (freeboard) and the lower dense region where the solid distribution is uniform. As the size and density of particles decrease, the entrainment of particles into the freeboard due to the rising gas bubbles is appreciable and particles are dispersed throughout the reactor, but the solid concentration, in general, decrease exponentially with the axial position. The particles are suspended by momentum transferred from the gas phase to the solid phase through the liquid medium. When very small and/or light particles are used, the effect of setting velocity is insignificant. A uniform distribution over the reactor is expected and the solid dispersion coefficient is very close to that of liquid.

As mentioned above, according to the axial profile of solid concentration, the cocurrent three-phase reactors with liquid as continuous phase can be classified into three types: (a) gas-sparged slurry reactors, (b) three-phase bubble columns, and (c) three-phase fluidized beds, as shown in Fig. 1. In the gas-sparged slurry reactor solid-liquid suspension can be regarded as a pseudo-homogeneous fluid and solid particles are distributed almost uniformly in the bed. The three-phase bubble column is characterized by an exponential decay of solid concentration from the bottom to top of the bed. The solid particles are suspended by liquid circulation induced by rising gas bubbles. On the other hand, in the three-phase fluidized bed solid particles are fluidized by both gas and liquid, and the bed is divided into two regions such as freeboard and dense regions. Based upon the authors' experiment by using 10 sizes of glass beads and 8 sizes of alumina particles, it was found that the substantial factors affecting the solid concentration are particles size and the density difference between solid and liquid.

In order to establish the criteria for the classification, experimental data as well as literature data on solid concentration profiles previously published were collected and plotted on the map given by two axes: particle size d_p and density difference between solid and liquid $(\rho_s-\rho_l)$as shown in Fig. 2. Three symbols, i.e., triangle, square and circle represent respectively, (a) gas-sparged slurry reactor (GSSR), (b) three-phase bubble column (TPBC), and (c) three-phase fluidized bed (TPFB). The open signs corresponds to the author's experimental results, and the solid signs to data published in the literatures. In addition, the

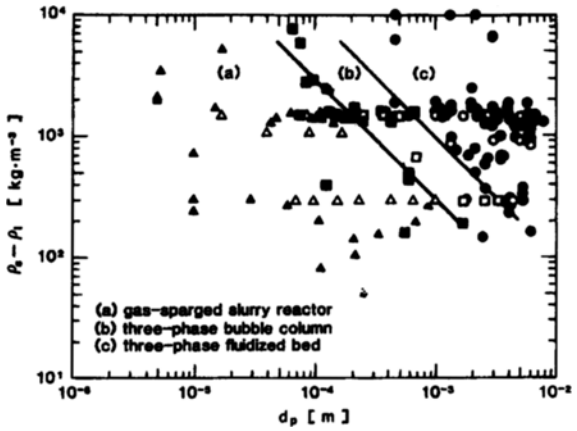

Fig. 2. Classification map for three-phase reactors. Open and closed signs stand for our results and data previously published, respectively.
(a) triangles: gas-sparged slurry reactors, (b) squares: three-phase bubble columns, (c) circles: three-phase fluidized beds.

experimental conditions in the literatures were summarized in Table 1. In Fig. 2, it is shown that all the data are divided clearly into three regions. The boundaries between (a) and (b) regions, and (b) and (c) regions can be represented by two straight lines of which the slope is −1. Then, they are given respectively by:

(a)-(b) boundary

$$d_p(\rho_s-\rho_l) = 0.3$$

(b)-(c) boundary

$$d_p(\rho_s-\rho_l) = 1.0$$

Thus, the criteria for three-phase reactors are expressed with:

(a) gas-sparged slurry reactors: $d_p(\rho_s-\rho_l)<0.3$
(b) three-phase bubble columns: $0.3<d_p(\rho_s-\rho_l)<1.0$
(c) three-phase fluidized beds: $1.0<d_p(\rho_s-\rho_l)$

Although the literature data contains the various experimental conditions as can be seen in Table 1, the criteria of classification were obtained in Fig. 2. This confirms that the dominant factors which affect the axial dispersion characteristics of solid particles are particle size and density difference between solid and liquid. The effects of other factors such as gas velocity, surface and interfacial tensions, liquid velocity, etc., are insignificant. On the other hand, liquid velocity has much effect on the axial distribution of solid particles especially for small particle systems.

GAS HOLDUP

The gas holdup is one of the most important factors for the reactor design, which depends on many variables, such as: geometrical characteristics of the reactor, type of distributor, physical properties of each phase and the operating conditions.

The authors' research work [Kim, 1987, 1988] clearly showed that the dependence of gas holdup on particle size and solid concentration was entirely different in three different types of

Table 1. Experimental conditions of hydrodynamic studies in three phase reactors

Authors	Particles	d_p [mm]	ρ_s [kg/m^3]	Gas	Liquid
(a) Gas-sparged slurry reactors					
Capuder & Koloini [1984]	$Ca(OH)_2$	0.010-0.015	2240	CO_2-air	water
	$CaCO_3$		2710		
Deckwer et al. [1980]	Al_2O_3	<0.005	2750	N_2	paraffin, xylenen decalin, kogaa-sin
Imafuku et al. [1968]	glass spheres	0.0642, 0.0743	2550	air	water+glycerine
	ion-exchange resin	0.11	1200		
Kara et al. [1982]	mineral ash	0.01	1300	air	water
	coal	0.03-0.07	1300		
Kato et al. [1972]	glass spheres	0.075-0.163	2520	air	water
Kawamura et al. [1965]	C_6H_5COOH	0.06	1270	air	water
	$CaCO_3$	0.015	2710		
	$BaCO_3$	0.0053	4430		
	PbI_2	0.017	6160		
Kelkar et al. [1984]	polystyrene beads	0.3	1006	air	water+CMC, triton 114
	oil shale	0.044-0.254	2300		
Seda et al. [1986]	$Ca(OH)_2$	0.007	2240	O_2, N_2	water+Na_2SO_4, NaCl, KCl
	glass beads	0.04, 0.096	2480		
	nylon 6 particle	2	1140		
Sanger & Deckwer [1981]	ion-exchange resin	0.115-0.875	1082-1269	air	water+glycol, PEG, glucose
Schumpet et al. [1987]	activated carbon	0.0054	1800	air	water+Na_2SO_4, Na_2SO_3
	kieselguhr	0.0066	2360		
	aluminium oxide	0.0081	3180		
Smith & Ruether [1985]	glass beads	0.0965, 0.0485	2420	N_2	water+methanol
		0.0485	3990		
Yasunishi et al. [1986]	glass beads	0.16	2500	air	water+glycerol
(b) Three-phase bubble reactors					
Capuder & Koloini [1984]	sand	>0.4	2580	CO_2-air	water
Fan et al. [1987]	glass beads	0.330, 0.460	2500	air	water
Heck & Onken [1987]	glass beads	0.308	2440	air	water
Imafuku et al. [1968]	glass beads	0.11, 0.18	2550	air	water+glycerine
	$FeSiO_2$	0.0735	7000		
	Cu	0.0645	8800		
Kojima & Asano	glass beads	0.115-0.425	2390-2490	air	water+glycerol
	acryl	1.7	1200		
Roy et al. [1964]	coal	0.063	1440	air	water+alcohol
	quartz	0.131-0.675	2630		light diesel oil
	Ni-Al Alloy	0.127	3466		til oil
	F. T. catalyst	0.347	2601		compressor oil
Smith & Ruether [1985]	glass spheres	0.1935	2420	N_2	water+ethanol
		0.0965	3990		
Yasunishi et al. [1986]	glass beads	0.16	2500	air	water+glycerol
(c) Three-phase fluidized reactors					
Alarez-Cuenca et al. [1983]	glass beads	1, 3, 5	2,480-2,950	air	water
Baker et al. [1978]	glass beads	1, 3, 5	2,484-2,955	air	water
Begovich & Watson [1978]	alumina	6.2	1,990	air	water
	glass beads	4.6	2,240		
	alumina-silicate	1.9	1,720		
	plexiglass	6.3	1,170		
	glass	6.2	2,200		

Table 1. Continued

Authors	Particles	d_p [mm]	ρ_s [kg/m^3]	Gas	Liquid
Blumn & Toman [1977]	catalyst	3.53	1,245-1,290	N_2	light mineral oil
	catalyst	4.23, 5.41	865-1,038		
Bruce & Revel-Chion	glass spheres	2, 4, 6, 8	2,360-2,750	air	water
Catros et al. [1985]	glass beads	3	2,253	air	water
Chiu & Ziegler [1985]	glass spheres	1, 3	2,670, 2,830	air	water
	γ-alumina	3.49-5.33	1,975-2,031		
Dakshinamurty et al. [1971]	rockwool shot	1.3	2,700, 11,000	air	water, kerosene
	sand	1.06, 2.235	2,700, 2,710		
	glass beads	3.348, 6.844	2,400		
	glass ball	4.89	2,260		
	iron shot	3	7,707		
Dakshinamurty et al. [1972]	glass ball	4.18-6.03	2,448	air, N_2	water, electrolyte
	glass beads	3.35, 6.84	2,420, 2,470		
	lead shot	2.13	11,175		
	rockwool shot	1.3	2,700		
Dhanuka & Stepanek [1980]	glass beads	1.98-5.86	2,960	CO_2	water+Na_2CO_3, $NaHCO_3$
Fan et al. [1987]	glass beads	0.778-6.11	2,200-2,876	air	water
Jean & Fan [1986]	glass beads	3.04-6.11	2,200-2,525	air	water
	alumina beads	2.27-6.69	3,644-3,690		
	lead particles	3.33	11,075		
Kato et al. [1985]	glass spheres	0.52-5.2	2,520	air	water
	porous alumina	1.5	1,800		
Capuder & Koloini [1984]	sand	>0.4	2580	CO_2-air	water
Kim et al. [1975]	glass beads	1.6	2,300, 2,520	air	water+acetone
	gravel	2.6	2,950		sugar, CMC
Kim & Kim [1983]	glass beads	1.7, 3.0, 6	2,500		water+glycerol, CMC, methanol, Triton, X-100
Lee & Al-dabbagh [1978]	glass beads	4.03, 6.08	2,560-2,590	air	water
Morooka et al. [1982]	glass beads	0.58-2.2	2,500	air	water
Muroyama et al. [1984]	glass beads	0.61-6.9	2,500	air	water
	activated carbon	1.8, 3.9	1,300		
	alumina beads	2	3,550		
Nikov & Delmas [1987]	plastic spheres	10	1,340	N_2	water+NaOH
	glass spheres	3, 10	2,520, 2,560		$K_3Fe(CN)_6$
	brass spheres	3	8,150		$K_4Fe(CN)_6$
Saberian-Broudjenni et al. [1985]	glass beads	1.37	2,640	air	water, gas oil
	porous alumina	2.15, 2.65	1,380-2,145		cyclohexane
					kerosene, C_2Cl_4
Soung [1978]	Co-Mo catalyst	2.79-3.79	1,370-1,390	N_2	heptane

three-phase reactors discussed above (GSSR, TPBC and TPFB). As shown in Fig. 3 and Fig. 4, the gas holdup increases with particle size in GSSR and TPFB, but decreases in TPBC. In GSSR the gas holdup decreases with increase of solid concentration. This effect is more pronounced at lower solid concentration. On the other hand, in TPFB and TPBC it was found that the increase of solid concentration does not reduce gas holdup.

From the observation of the hydrodynamic state in this range of gas velocity the transition from homogeneous bubbly flow to heterogeneous churn-turbulent flow was found at the gas velocity 0.04-0.06 m/s. It was interesting to note that the critical gas velocity for this transition was substantially independent of particle size and solid concentration even for the case of porous alumina and coal particles system.

Zuber and Findlay [1965] developed a theory to calculate the gas holdup for churn-turbulent flow regime. The equation is given by

$$U_g/\varepsilon_g = C_0(U_g + U_l) + V_{b0}$$

When the liquid is fed batchwise, the value of U_l is zero, and C_0 is a distribution parameter representing a nonuniformity of radial distribution and V_{b0} represents free rising velocity of a single bubble.

Fig. 5 shows plots of U_g/ε_g against U_g for glass beads system. For each size of particle the data can be expressed by a single straight line with the gradient C_0 and the intercept V_{b0} in the

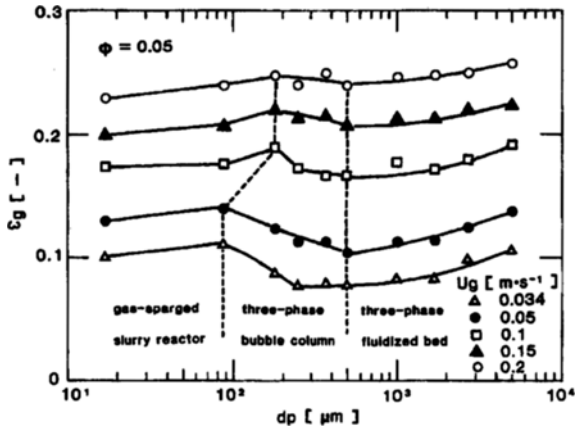

Fig. 3. Relationship between particle size and gas holdup by changing gas velocity (glass beads system).

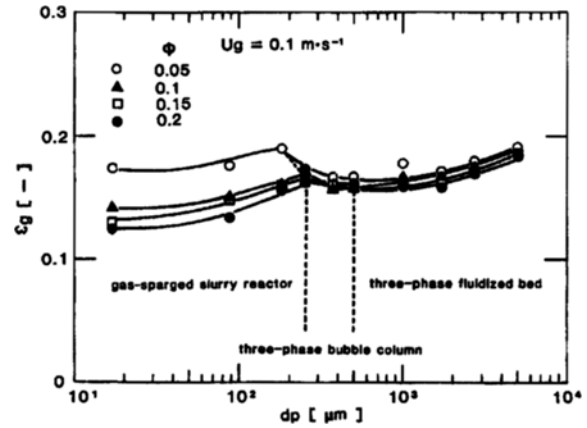

Fig. 4. Effect of particle size on gas holdup with respect to solid content (glass beads system).

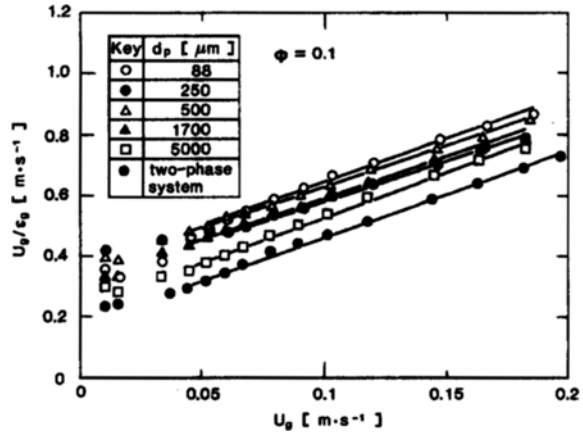

Fig. 5. Relationship between U_g/ε_g and U_g for glass beads system.

churn turbulent flow regime (U_g>0.04-0.06 m/s). Similar plots can be obtained for other particle systems. For two-phase system, where no solid particles exist, the values of C_0' and V_{b0}' were 2.67 and 0.203 m/s, respectively.

To elucidate the effects of particle size and solid concentration, C_0/C_0' were plotted against particle size as a function of

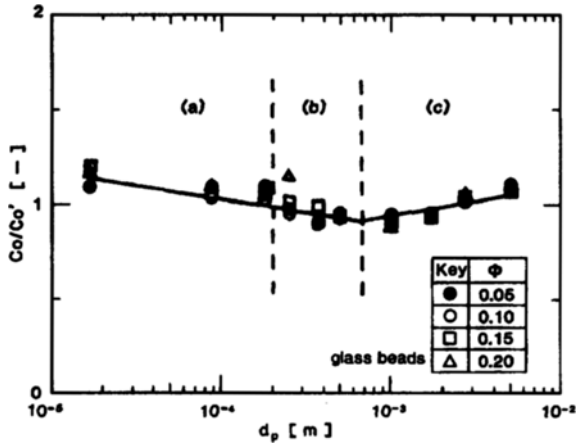

Fig. 6. Effects of particle size and particle concentration on C_0/C_0' for glass beads system.

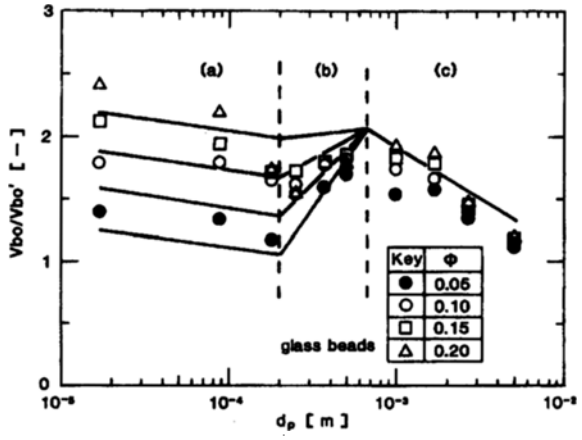

Fig. 7. Effects of particle size and particle concentration on V_0/V_{b0}' for glass beads system.

solid concentration for glass beads system, as shown in Fig. 6. There was only a slight decrease with particle size in both gas-sparged slurry reactors and three-phase bubble columns, whereas an increase in three-phase fluidized beds. In addition, the value of C_0 was found to be independent of solid concentration.

Fig. 7 shows the relationship between V_{b0}/V_{b0}' and particle size for glass beads system. It was found that the dependence of the value of V_{b0} on particle size is different in each type of reactors. The increase in particle size causes a predominant decrease of V_{b0} in both gas-sparged slurry reactors and three-phase fluidized beds. On the contrary, in three-phase bubble columns the opposite tendency was observed. The value of V_{b0} in both gas-sparged slurry reactors increases strongly with solid concentration, but this effect was negligible in three-phase fluidized beds.

Considering that the parameter $d_p(\rho_s-\rho_l)$ may characterize the hydrodynamics of three-phase reactors, data on C_0/C_0' and V_{b0}/V_{b0}' for three different particles system were plotted against $d_p(\rho_s-\rho_l)$, as shown in Fig. 8 and Fig. 9, respectively. Both C_0 and V_{b0} were found to be well correlated with $d_p(\rho_s-\rho_l)$ and solid concentration ϕ:

(a) gas-sparged slurry reactor

$$C_0/C_0' = 0.96 - 0.114 \log[d_p(\rho_s-\rho_l)]$$

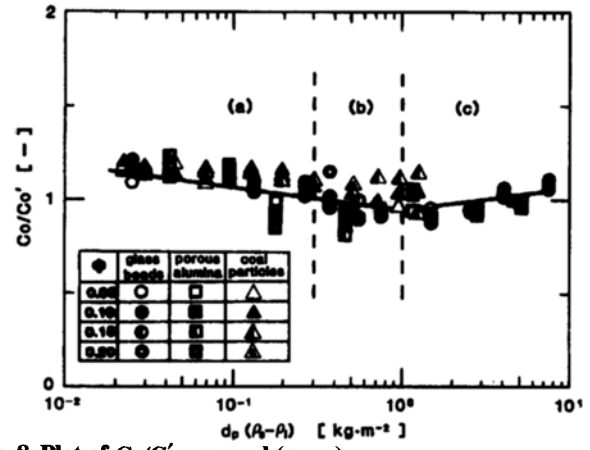

Fig. 8. Plot of C_0/C_0' versus $d_p(\rho_s-\rho_l)$.

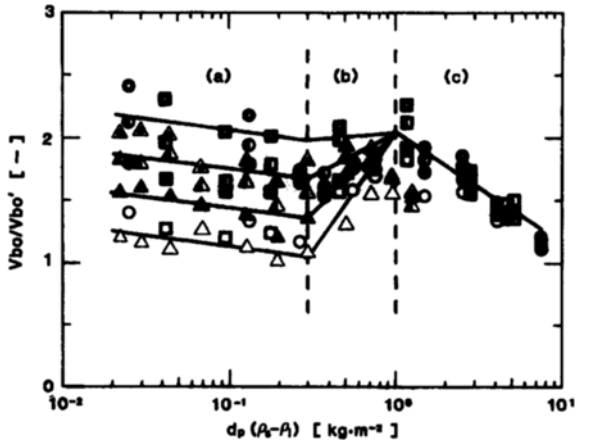

Fig. 9. Plot of V_{b0}/V_{b0}' versus $d_p(\rho_s-\rho_l)$.

$$V_{b0}/V_{b0}' = 0.723+6.19\phi-0.137\ \log[d_p(\rho_s-\rho_l)]$$

(b) three-phase bubble columns

$$C_0/C_0' = 0.96-0.114\ \log[d_p(\rho_s-\rho_l)]$$

$$V_{b0}/V_{b0}' = 2.05+(2.51-11.84\phi)\ \log[d_p(\rho_s-\rho_l)]$$

(c) three-phase fluidized beds

$$C_0/V_0' = 0.95+0.105\ \log[d_p(\rho_s-\rho_l)]$$

$$V_{b0}/V_{b0}' = 2.04-0.843\ \log[d_p(\rho_s-\rho_l)]$$

Thus the gas holdup can be calculated by the above correlations when C_0' and V_{b0}' and for gas-liquid system are known.

MASS TRANSFER

1. Background

The volumetric mass transfer coefficient is also recognized as one of the important parameters for a proper design of three-phase reactors. The presence of solid particles can significantly affect mass transfer characteristics. Many experimental studies of the solid particle effects on the mass transfer in three-phase reactors have been conducted comprehensively but most of them covered only narrow ranges of particle size.

In the case of large and heavy particle systems, both the volumetric liquid-phase mass transfer coefficient, k_la, and the gas-liquid interface area, a, are larger than those in two-phase systems. Østergaard and Fosbøl [1972] reported that k_la in beds of 6,000 μm glass ballotini is higher than that in beds of 1,000 μm particles, and k_la in two-phase bubble column is of intermediate magnitude. Similar results are also reported by Nguyen-Tien et al. [1985].

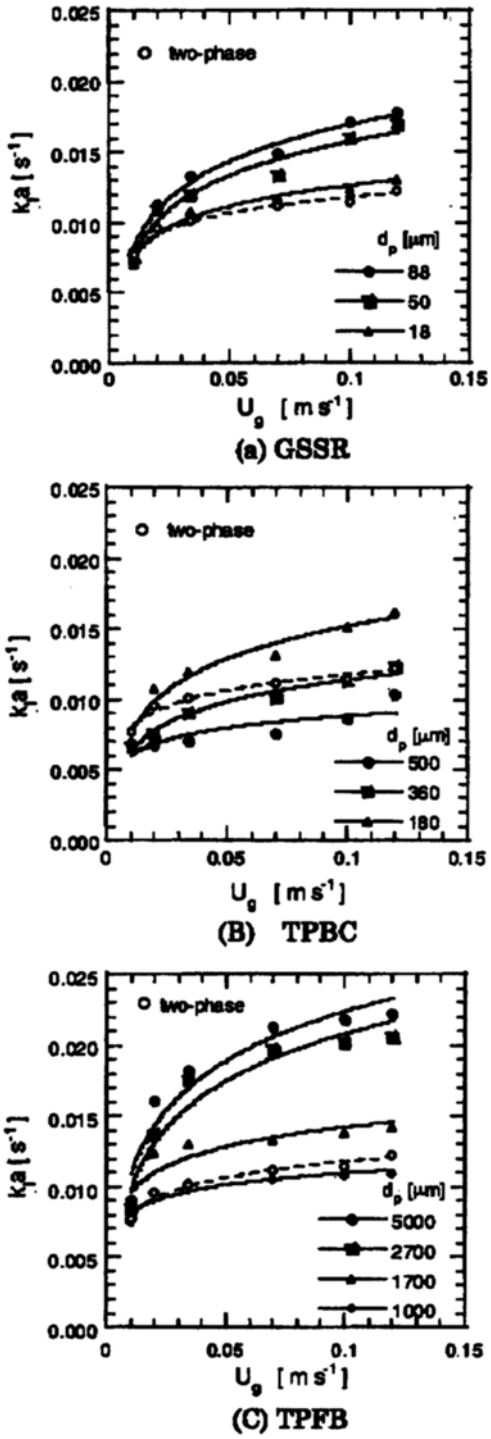

Fig. 10. Dependence of volumetric gas-liquid mass transfer coefficient k_la on superficial gas velocity.

For small particle systems, the contradictory results have been reported with respect to the effect of solid particles on gas-liquid mass transfer and gas holdup. Using glass beads of 60-270 μm Koide et al. [1989] reported that the presence of suspended solid particles reduces values of k_la and ε_g. On the other hand, Nguyen-Tien et al. [1987] found a noticeable increase of k_la in 50 μm particles systems at low solid concentration, compared with that in two-phase systems. They suggested that the particles increase the liquid-side mass transfer coefficient by penetrating into liquid-side diffusion film. Sada et al. [1987] also showed that both k_l and a in three-phase systems are larger than those in two-phase systems.

2. Effects of Particle Size and Solid Concentration on Mass Transfer

The mass transfer characteristics in three-phase reactors with various sizes of particles ranging from 18 to 5,000 μm have studied for three types of three-phase reactors, i.e. GSSR, TPBC and TPFB [Charinpanitkul et al., 1993].

Figs. 10(a), (b) and (C) shows k_la plotted against the superficial gas velocity in GSSR, TPBC and TPFB, respectively. In all cases, at gas velocity below 0.05 $m \cdot s^{-1}$ small bubbles were observed to disperse uniformly in the column (bubbly flow regime). In this regime, the population of bubbles increases linearly with gas velocity, leading to growing gas-liquid interfacial area. Thus, the values of k_la increase considerably with gas velocity.

When gas velocity was increased above 0.05 $m \cdot s^{-1}$, the bubble size became larger and the coalescence took place, i.e., churn-turbulent flow appeared. In spite of an increase in gas holdup no significant change in gas-liquid interfacial area appeared because of large bubble sizes. The influence of gas velocity on mass transfer is not so significant at high gas velocities above 0.05 $m \cdot s^{-1}$.

It is evident that the values of k_la in three-phase systems were larger than that in two-phase systems except for 360-1,000 μm glass beads systems. In particular, large particle systems (2,700 and 5,000 μm glass beads) exhibit a remarkable increase in k_la. These trends are consistent with the results reported by Nguyen-Tien et al. [1985].

The effect of particle size, d_p, on k_la is shown in Fig. 11. In the case of TPBC, k_la decreased with increasing the size of glass beads particle, while increasing in the case of GSSR and TPFB. The value of k_la, therefore, has a maximum at a particle size of 88-180 μm and a minimum at 500-1,000 μm.

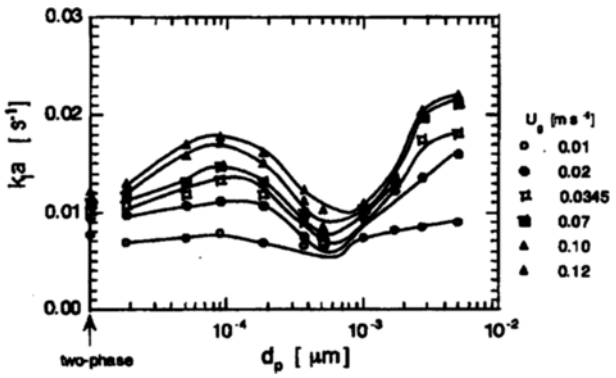

Fig. 11. Effect of particle size on k_la at solid concentration of 0.10.

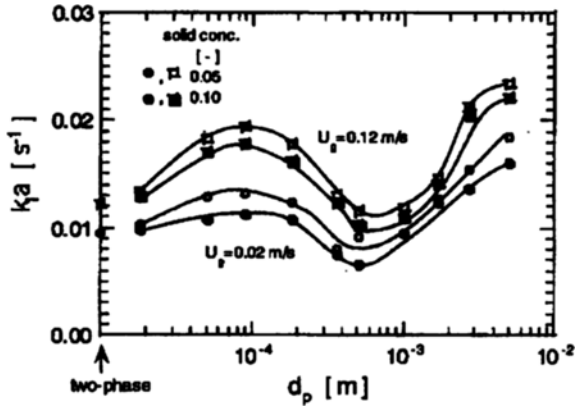

Fig. 12. Effect of solid concentration on k_la.

The effect of solid concentration on mass transfer is shown in Fig. 12. It was found that the value of k_la decreases significantly with solid concentration in the case of GSSR, whereas the same effect on k_la is less pronounced in the case of TPBC and TPFB.

In a word, the effect of glass beads size and concentration on the mass transfer coefficient are notably different in three types of three-phase reactors.

BUBBLE CHARACTERISTICS

Both the gas holdup and mass transfer rate are directly dependent on the bubble characteristics such as bubble size, size distribution and bubble frequency.

By using a dual optical fiber probe system, Kim [1989] measured the bubble length and bubble frequency in a cocurrent three-phase reactor. The experimental results indicated that the effect of particle size on bubble length appears to be different in three types of three-phase reactors. As shown in Fig. 13, the bubble length decreases with particle size in both GSSR and TPFB. On the contrary, in TPBC the increase in particle size causes enlargement of bubble size. It is suggested that the increase of particle size may cause bubble break-up in former two types of reactors, but rather coalescence in the last type of re-

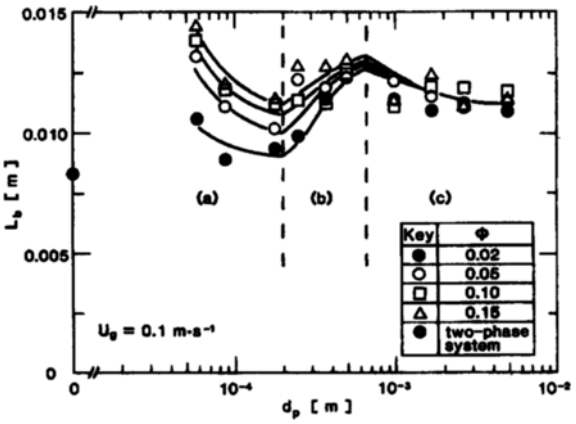

Fig. 13. Effect of particle size on bubble length at various solid concentrations.

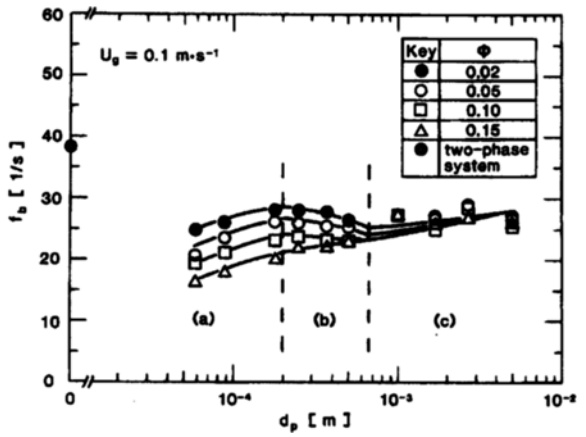

Fig. 14. Effect of particle size on bubble frequency at various solid concentration.

actors. The presence of particles promotes bubble coalescence, resulting in the increase of bubble length in all types of three-phase reactors compared to two-phase reactors. It was evident that the solid concentration gives considerable effects on bubble length in different way in three types of reactors.

Fig. 14 shows the bubble frequency in relation to particle size and solid concentration. It can be seen that the effect of particle size on bubble frequency is contrary to that on bubble length as previously shown in Fig. 13. There was an increase of bubble frequency with an increase in particle size in both GSSR and TPFB, while a decrease in TPBC. The dependence of bubble frequency on the solid concentration was reduced with an increase in particle size as in the case of bubble length.

As the particle size increases, the promotion of bubble coalescence due to the presence of solid particles becomes more pronounced in TPBC, whereas both TPFB and GSSR show an opposite trend. Therefore, the gas holdup increases with particle size in GSSR and TPFB, but decreases in TPBC. Accordingly, one can infer that bubble coalescence is intensified in the transient region between GSSR and TPFB, then a decrease in gas-liquid interfacial area exceeds an increase in k_l, resulting in a reduction of k_la. Moreover, the presence of solid particles can be considered to reduce the gas-liquid interfacial area. Therefore, an increase in k_la in three-phase reactors is considered to be mainly attributable to increasing the value of k_l. Large bubbles become more irregular in shape and unsteadily oscillate, leading to an increase in k_l. In addition, large bubbles enhance circulation flow of liquid phase because of high rise velocity and turbulent motion. This effect also enhances the gas-liquid mass transfer rate.

SOLID CONCENTRATION PROFILES PREDICATED BY A WAKE SHEDDING MODEL

As discussed above, both hydrodynamic and transport characteristics of three-phase reactors considerably depend on the type of three-phase reactors classified based on the solids distribution along the reactor. Thus, it is essential to study the mechanism of the solid concentration profile development.

Considerable efforts have been made toward the quantitative description of the axial solid distribution. Most of them have been based on the sedimentation-dispersion model that was originally proposed by Cova [1966] and Suganuma and Yamanishi [1966]. The model considers a solids axial dispersion flux and a solids sedimentation flux superimposed on the average slurry convection flux. For the batch mode with respect to solids and liquids the sedimentation-dispersion model gives the expression of the axial solid distribution as

$$C_f = C_{f0} \exp(-v_t/E_p \cdot z) \quad (1)$$

where v_t is the hindered settling velocity and E_p the solid axial dispersion coefficient. This model can describe the solid particle behavior successfully. However, the physical meaning of two parameters in the model is unclear and there are some discrepancies in their interpretation [Jean et al., 1989; de Bruijn et al., 1989]. The parameters in the sedimentation-dispersion model, i.e., v_t and E_p, are not obtained independently, but given as the ratio v_t/E_p from empirical fitting of the model with data relating C_f to z at steady state conditions. Consequently, the sedimentation-dispersion model must be regarded as being phenomenological and merely a one-parameter empirical correlation.

A mechanistic approach to the analysis of the axial solid mixing can provide a fundamental understanding of hydrodynamic phenomena. The solids mixing behavior inherently depends on the turbulent dispersion induced by rising gas bubbles and the entrainment due to the bubble wake motion. In the churn-turbulent flow regime the particle entrainment due to the bubble wake motion is considered to be the predominant mechanism responsible for the upward motion of particles.

1. Mechanism of Particle Entrainment by Bubble Wake

As the gas bubble is initially introduced into the bed the wake is developed almost instantly, transported upwards behind the rising bubble at the same velocity. After travelling a short distance the wake is shed into the slurry phase and then the reformation of the wake takes place immediately. The wake carries solid particles and liquid elements at a velocity greater than the average liquid velocity. Since the solid concentration in the wake is lower than that in the slurry phase, the wake entrains some amount of liquid upwards, resulting in the longitudinal decay of solid holdup.

2. Wake Shedding Model

The bed consists of a gas phase, a wake phase and a slurry phase. For simplification batch operation with respect to solids and liquids is assumed here. The bubbles and their wakes are assumed to travel at the same velocity. The holdups of gas, wake and slurry phases, ε_g, ε_w, ε_f, are assumed to be constant at any cross section of column. From the definition of individual holdups, the following expression can be written:

$$\varepsilon_g + \varepsilon_f + \varepsilon_w = 1 \quad (2)$$

The solid concentration in slurry phase $C_f(z)$ can be expressed as a function of the height z. There is assumed to be no particle exchange between wake and slurry phases except at the shedding and formation of wake. The wake is shed from the bubble after travelling a constant distance. The vertical distance traveled, "wake shedding length," is defined to be *l*. The

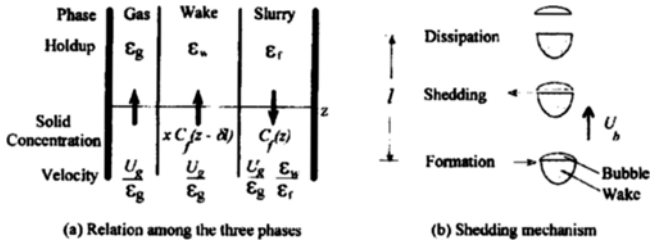

Fig. 15. Wake shedding model.
(a) Relation among the three phases, (b) Shedding mechanism.

model is schematically illustrated in Fig. 15.

At a certain level z the average travelling distance of bubble wake passing through the column cross section from the formation point can be denoted by δl, which satisfies the following equation

$$\frac{1}{l}\int_{z-l}^{z} C_f(z)dz = C_f(z-\delta l) \tag{3}$$

The ratio of solid concentration in the wake to that in slurry phase at the height where wake formation takes place is defined to be x. The solid concentration in wake phase at the level z is given by

$$C_w = xC_f(z-\delta l) \tag{4}$$

Thus, the upward mass flux of solid particles due to the entrainment by the wake is given by

$$F_w = xC_f(z-\delta l)\frac{U_g}{\varepsilon_g}\varepsilon_w \tag{5}$$

In order to satisfy the mass balance the downward velocity of solid particles in slurry phase is given by

$$U_f = \frac{U_g}{\varepsilon_g}\frac{\varepsilon_w}{\varepsilon_f} + v_p \tag{6}$$

where v_p is the particle settling velocity. Thus, the downward mass flux of solid particles through the slurry phase is given by

$$F_f = C_f(z)\left(\frac{U_g}{\varepsilon_g}\frac{\varepsilon_w}{\varepsilon_f} + v_p\right)\varepsilon_f \tag{7}$$

Since the mass balance of solid particles at any cross section of column is satisfied for steady-state flow conditions, combination of Eqs. (5) and (7) yields,

$$\frac{x}{1+\dfrac{v_p}{(U_g/\varepsilon_g)(\varepsilon_w/\varepsilon_f)}}C_f(z-\delta l) = C_f(z) \tag{8}$$

By taking logarithms of both sides of Eq. (8) and differentiating with respect to z, the following differential equation is obtained

$$\frac{C_f'(z-\delta l)}{C_f(z-\delta l)} = \frac{C_f'(z)}{C_f(z)} \tag{9}$$

With the solid concentration at the bottom of the column, C_{f0}, the solution of Eq. (9) is given as follows

$$C_f(z) = C_{f0}\exp\left(\frac{\log\alpha}{\delta l}z\right) = C_{f0}\exp(-\beta z) \tag{10}$$

where

$$\alpha = \frac{x}{1+\dfrac{v_p}{(U_g/\varepsilon_g)(\varepsilon_w/\varepsilon_f)}} \tag{11}$$

and

$$\beta = -\frac{\log\alpha}{\delta l} \tag{12}$$

Introducing a parameter, k, defined by

$$k = \frac{\varepsilon_w}{\varepsilon_g} \tag{13}$$

and combining Eq. (2) and (13) gives

$$\frac{\varepsilon_w}{\varepsilon_f} = \frac{k\varepsilon_g}{1-\varepsilon_g-k\varepsilon_g} \tag{14}$$

Substituting Eq. (14) into Eq. (11) gives

$$\alpha = \frac{x}{1+\dfrac{v_p}{kU_g/(1-\varepsilon_g-k\varepsilon_g)}} \tag{15}$$

Since the axial solid concentration distribution can be regarded as a linear function for a short distance provided the exponential term β is relatively small, the value of δ in Eq. (3) can be assumed to be 0.5.

3. Discussion

The wake shedding model involves three parameters, k, l and x. From the model deduction, it is indicative that the ratio of solid concentration in wake phase to that in slurry phase height (x) plays a very important role in determining the axial solid concentration profiles. If x is equal to unity or close to zero, the other two parameters do not influence the axial solid concentration profile. Therefore, x is considered to be the governing parameters for predicating the axial solid concentration profile.

Although several studies have been made on the solid concentration in the literature [Kitano and Fan, 1988; Tsutsumi et al., 1988; Kreischer et al., 1990; Song et al., 1991], there is little agreement so far. Therefore, the values of x were obtained directly from fitting the model to experimental data [Tsutsumi et al., 1987] as well as published data on the axial solid concentration profiles.

Considering the process of particle trapping into the bubble wake region, the effect of particle size and density on the solid concentration in the wake phase can be described qualitatively as follows: when the particle size is very small and the density of solid approaches that of the liquid, the particles can be regarded as a tracer of the liquid motion so that the solid concentration in the bubble wakes is considered to be same as that in the slurry. On the other hand, when the particle size and density difference ($\rho_s-\rho_l$) increase, the particle is more difficult to follow the liquid flow because of its large inertia, and thus the solid concentration in the bubble wake decreases. When the interia of the particle is larger enough, the solid concentration in the bubble wake approaches zero.

As mentioned in the previous section, the axial solid concentration profile can be characterized by density difference ($\rho_s-\rho_l$)

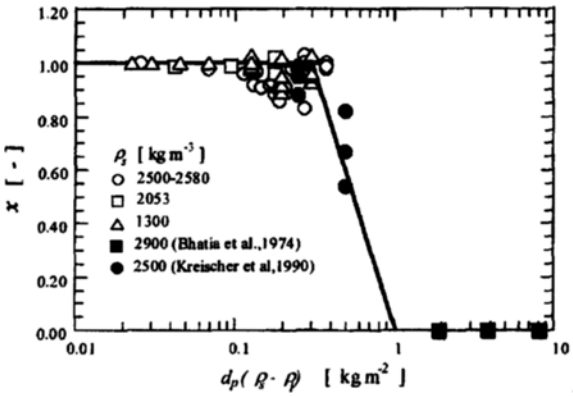

Fig. 16. Relation between x and $d_p(\rho_s-\rho_l)$.

and particle size d_p. Accordingly, the relative solid concentration x was plotted versus $d_p(\rho_s-\rho_l)$ in Fig. 16. It is noteworthy that the values of x did not exceed unity for most of particle systems. This result indicates that the solid concentration in wake phase is not greater than that in slurry phase. In the case of small and/or light particle systems the value of x was found to be equal to unity independent of particle size. For x=1 the value of β is close to zero, indicating that particles are distributed almost uniformly.

For large particle systems the value of x became less than unity and gradually decreased with the increase in particle size. Both the decrease in x and the increase in particle settling velocity raise the value of β significantly, leading to a considerable drop in solid concentration from the bottom to the top.

From Fig. 16, the relationship between x and particle size and density can be correlated by:

$$d_p(\rho_s-\rho_l)\leq 0.3;\ x = 1.0 \tag{21}$$

$$0.3<d_p(\rho_s-\rho_l)<1.0;\ x=-1.912\log[d_p(\rho_s-\rho_l)] \tag{22}$$

$$1.0<d_p(\rho_s-\rho_l);\ x=0 \tag{23}$$

The above correlations are fairly consistent with the criteria for classification of three types of three-phase reactors. In the gas-sparged slurry reactor, where very small and light particles are used, the solid concentration in wake phase is almost same as that in slurry phase. The significant particle entrainment by bubble wake leads to the uniform axial solids distribution. When the solid particles become larger and heavier, the solid concentration in bubble wake gradually decreases and the wake entrains fewer particles resulting in the axial decay of solid holdup. This is the case of three-phase bubble columns. In the three-phase fluidized beds, the particles are too large and heavy to follow the motion of liquid. Therefore, the solid concentration in bubble wakes is near zero and two regions, i.e. freeboard and dense regions, can be clearly observed in such reactors.

CONCLUDING REMARKS

Cocurrent upward three-phase reactors with discontinuous gas phase can be classified into three types according to the axial solid concentration profile: (a) gas-sparged slurry reactors, (b) three-phase bubble columns and (c) three-phase fluidized beds. Hydrodynamic and transport characteristics of three-phase reactors were found to depend on the type of reactors. The gas holdup, bubble characteristics and mass transfer rate show the different dependency of particle size, solid concentration and gas velocity in each type of three-phase reactors.

The wake shedding model was proposed for describing the axial solid concentration profiles in three-phase reactors. A mechanistic analysis of particle entrainment by bubble wake indicates the relative solid concentration in bubble wake phase is the dominant factor for predicating the solid holdup.

On the basis of the experimental data, the correlations for the relative solid concentration in wake phase (x) in three types of three-phase reactors were obtained as a function of $d_p(\rho_s-\rho_l)$:

(a) gas sparged slurry reactors

$d_p(\rho_s-\rho_l)\leq 0.3;\ x=1.0$

(b) three-phase bubble column

$0.3<d_p(\rho_s-\rho_l)<1.0;\ x=-1.912\log[d_p(\rho_s-\rho_l)]$

(c) three-phase fluidized bed

$1.0<d_p(\rho_s-\rho_l);\ x=0$

NOMENCLATURE

a : gas-liquid interfacial area [m^{-1}]
C(z) : solid concentration at height z [$kg\cdot m^{-3}$]
C_0 : solid concentration at the bottom of column [$kg\cdot m^{-3}$]
d_b : bubble diameter [m]
d_p : particle size [m]
E_p : solid axial dispersion coefficient [$m^2\cdot s^{-1}$]
F : void function
F_f : downward mass flux of solid particles [$kg\cdot m^{-2}\cdot s^{-1}$]
F_w : upward mass flux of solid particles [$kg\cdot m^{-2}\cdot s^{-1}$]
f_b : wake shedding frequency [s^{-1}]
g : gravitational acceleration [$m\cdot s^{-2}$]
k : ration of wake volume to bubble volume wake shedding length [m]
k_l : liquid-phase mass transfer coefficient [$m\cdot s^{-1}$]
k_la : volumetric liquid-phase mass transfer coefficient [s^{-1}]
l : wake shedding length [m]
Re : reynolds number
Sr_b : strouhal number
U_b : bubble rising velocity [$m\cdot s^{-1}$]
U_f : velocity of solid particles in slurry phase [$m\cdot s^{-1}$]
U_g : superficial gas velocity [$m\cdot s^{-1}$]
U_l : liquid velocity [$m\cdot s^{-1}$]
V_t : hindered settling velocity in sedimentation-dispersion model [$m\cdot s^{-1}$]
V_p : settling velocity of solid particles [$m\cdot s^{-1}$]
We : Weber number
x : ratio of solid concentration in wake phase to that in slurry phase height

Greek Letters

α : exponential term defined by Eq. (11)
β : parameter defined by Eq. (12) [m^{-1}]

δ : parameter in Eq. (3)
ε : holdup
ϕ : 4solid concentration
λ : ratio of the vortex traveling velocity to the bubble rise velocity
μ : viscosity [Pa·s]
ρ : density [kg·m^{-3}]
ρ_l : liquid density [kg·m^{-3}]
ρ_s : solid density [kg·m^{-3}]
θ_w : wake life after shedding [s]

Subscripts

b : bubble phase
f : slurry phase
g : gas phase
l : liquid phase
s : solid phase
w : wake phase

REFERENCES

Alvarez-Cuenca, M., Baker, C. G. J., Bergougnou, M. A. and Nerenberg, M. A., "Oxygen Mass Transfer in Three-phase Fluidized Beds Working at Large Flow Rates," *Can. J. chem. Engng*, **61**, 58 (1983).

Baker, C. G. J., Armstrong, E. R. and Bergougnou, M. A., "Heat Transfer in Three-phase Fluidized Beds," *Powder Tech.*, **21**, 195 (1978).

Begovich, J. M. and Watson, J. S., "Hydrodynamic Characteristics of Three-phase Fluidized Beds, in Fluidization," (Edited by Davidson, J. F. and Keairns, D. L.), Cambridge University Press, Cambridge, 190 (1978).

Bhatia, V. K. and Epstein, N., "Three-phase Fluidization: A Generalized Wake Model," In Proc. Int. Symp. Fluidization and its Applications, Toulouse (France): Editions Cepadues, 380 (1974).

Blum, D. B. and Toman, J. J., "Three-phase Fluidization in a Liquid Phase Methanator," *AIChE Symp. Ser.*, **73**(161), 115 (1977).

Bruce, P. N. and Revel-Chion, L., "Bed Porosity in Three-phase Fluidization," *Powder Tech.*, **10**, 243 (1974).

Capuder, E. and Koloini, T., "Gas Hold-up and Interfacial Area in Aerated Suspensions of Small Particles," *Chem. Engng Res. Des.*, **62**, 255 (1984).

Catros, A., Bernard, J. R., Briens, C. and Bergougnou, M. A., "Gas Holdup above the Bed Surface and Grid Gas Jet Hydrodynamics for Three Phase Fluidized Beds," *Can. J. chem. Engng*, **63**, 754 (1985).

Chang, S., Kang, K. Y. and Kim, S. D., "Mass Transfer in Two and Three-phase Fluidized Bed," *J. Chem. Eng. Japan*, **19**, 524 (1986).

Charinpanitkul, T., Tsutsumi, A. and Yoshida, K., "Gas-liquid Mass Transfer in a Three-phase Reactor," *J. Chem. Eng. Japan*, **26**(4), 440 (1993).

Chiu, T.-M. and Ziegler, E. N., "Liquid Holdup and Heat Transfer Coefficient in Liquid-solid and Three-phase Fluidized Beds," *AIChE Journal*, **31**, 1504 (1985).

Cova, D. R., "Catalyst Suspension in Gas-agitated Tubular Reactors," *Ind. Eng. Chem. Proc. Des. Dev.*, **5**, 20 (1966).

Dakshinamurty, P., Subrahmanyam, V. and Rao, J. N., "Bed Porosities in Gas-liquid Fluidization," *Ind. Engng Chem. Process Des. Dev.*, **10**, 322 (1971).

Dakshinamurty, P., Rao, K. V., Subbaraju, R. V. and Subrahmanyam, V., "Bed Porosities in Gas-liquid Fluidization," *Ind. Engng Chem. Process Des. Dev.*, **11**, 318 (1972).

de Bruijn, T. J. W., Reilly, I. G., MacIntyre, D. and Scott, D. S., "Solids Exit Discontinuity in Slurry Bubble Columns," *Can. J. Chem. Eng.*, **67**, 283 (1989).

Deckwer, W.-D., Louisi, Y., Zaidi, A. and Ralek, M., "Hydrodynamic Properties of the Fischer-Tropsch Slurry Process," *Ind. Engng Chem. Process Des. Dev.*, **19**, 699 (1980).

Deckwer, W.-D. and Schumpe, A., "Transport Phenomena in Three-phase Reactors with Fluidized Solids," *Ger. Chem. Eng.*, **7**, 168 (1984).

Dhanuka, V. R. and Stepanek, J. B., "Gas and Liquid Hold-up Drop Measurement in a Three-phase Fluidized Bed, Fluidization," Davision, J. F. and Keairns, D. L. eds, Cambridge Univ. Press, 179 (1978).

Dhanuka, V. R. and Stepanek, J. B., "Simultaneous Measurement of Interfacial Area and Mass Transfer Coefficient in Three-phase Fluidized Beds," *AIChE Journal*, **26**, 1029 (1980).

El-Temtarmy, S. A. and Epstein, N., "Contraction or Expansion of Three-phase Fluidized Beds Containing Fine/Light Solids," *Can. J. Chem. Eng.*, **57**, 520 (1979).

Epstein, N., "Three-phase Fluidization: Some Knowledge Gaps," *Can. J. Chem. Eng.*, **59**, 259 (1981).

Fan, L.-S., Jean, R.-H. and Kitano, K., "On the Operating Regimes of Cocurrent Upward Gas-liquid-solid Systems with Liquid as the Continuous Phase," *Chem. Eng. Sci.*, **42**, 1853 (1987).

Fan, L.-S. and Tsuchiya, K., "Bubble Wake Dynamics in Liquids and Liquid-Solid Suspensions," Butterworth-Heinemann Publisher, Stoneham, MA (1990).

Farkas, E. J. and Leblond, P. F., "Solids Concentration Profile in the Bubble Column Slurry Reactor," *Can. J. Chem. Eng.*, **47**, 215 (1969).

Fukuma, M., Muroyama, K. and Yasunishi, A., "Properties of Bubble Swarm in a Slurry Bubble Column," *J. Chem. Eng. Japan*, **20**, 28 (1987).

Heck, J. and Onken, U., "Hysteresis Effects in Suspended Solid Particles in Bubble Columns With and Without Draft Tube," *Chem. Eng. Sci.*, **42**, 1211 (1987).

Imafuku, K., Wang, T.-Y., Koide, K. and Kubota, H., "The Behavior of Suspended Solid Particles in the Bubble Column," *J. Chem. Eng. Japan*, **1**, 153 (1968).

Jean, R.-H. and Fan, L.-S., "A Simple Correlation for Solids Holdup in a Gas-liquid-solid Fluidized Bed," *Chem. Eng. Sci.*, **41**, 2823 (1986).

Jean, R.-H., Tang, W.-T. and Fan, L.-S., "The Sedimentation-dispersion Model for Slurry Bubble Columns," *AIChE Journal*, **35**, 662 (1989).

Kara, S., Kelkar, B. G. and Shah, Y. T., "Hydrodynamics and Axial Mixing in a Three-phase Bubble Column," *Ind. Eng. Chem. Process Des. Dev.*, **21**, 584 (1982).

Kato, Y., Nishiwaki, A., Kago, T., Fukuda, T. and Tanaka, S., "Gas Holdup and Overall Volumetric Absorption Coefficient in Bubble Columns with Suspended Solid Particles," *Int. Chem. Eng.*, **13**, 563 (1973).

Kato, Y., Morooka, S., Kago, T., Saruwatari, T. and Yang, S.-Z., "Axial Holdup Distributions of Gas and Solid Particles in Three-phase Fluidized Bed for Gas-liquid(slurry)-solid Systems," *J. Chem. Eng. Japan*, **18**, 308 (1985).

Kawamura, K., Sasano, T. and Mifune, A., "Solid-liquid Contact in a Gas-liquid-solid Fluidized Bed," *Kagaku Kogaku*, **29**, 693 (1965).

Kelkar, B. G., Shah, Y. T. and Carr, N. L., "Hydrodynamics and Axial Mixing in a Three-phase Bubble Column," *Ind. Engng Chem. Process Des. Dev.*, **23**, 308 (1984).

Kim, S. D., Baker, C. G. J. and Bergougnou, M. A., "Phase Holdup Characteristics of Three Phase Fluidized Beds," *Can. J. chem. Engng.*, **53**, 134 (1975).

Kim, S. D. and Kim, C. H., "Axial Dispersion Characteristics of Three Phase Fluidized Beds," *J. Chem. Eng. Japan*, **16**, 172 (1983).

Kim, Y. H., Tsutsumi, A. and Yoshida, K., "Effect of Particle Size on Gas Holdup in Three-phase Reactors," in Reactions & Reaction Engineering (Edited by Mashelkar, R. A. and Kumar, R.)," Indian Academy of Sciences, Bangalore, 261 (1987).

Kim, Y. H., Tsutsumi, A. and Yoshida, K., "Prediction of Gas Holdup for Three-phase Reactors," German/Japanese Symposium on Bubble Column, Schwerte, Germany, 129 (1988).

Kim, Y. H., Ph.D. Thesis, University of Tokyo (1989).

Kitano, K. and Fan, L.-S. "Near-wake Structure of a Single Gas Bubble in a Two-dimensional Liquid-solid Fluidized Bed: Solids Holdup," *Chem. Eng. Sci.*, **43**, 1355 (1988).

Kojima, H. and Asano, K., "Hydrodynamic Characteristics of Suspension-bubble Column," *Kagaku Kogaku Ronbunshu*, **6**, 46 (1980).

Koide, K., Takazawa, A., Komura, M. and Matsunaga, H., "Gas Holdup and Volumetric Liquid Phase Mass Transfer Coefficient in Solid-suspended Bubble Column," *J. Chem. Eng. Japan*, **17**, 459 (1984).

Kreischer, B. E., Moritomi, H. and Fan, L.-S., "Wake Solids Holdup Characteristics Behind a Single Bubble in a Three-dimensional Liquid-solid Fluidized Bed," *Int. J. Multiphase Flow*, **16**, 187 (1990).

Lee, J. C. and Al-Dabbagh, N., "Three-phase Fluidized Beds Onset of Fluidization at High Gas Rates," in Fluidization (Edited by Davidson, J. F. and Keairns, D. L.), Cambridge University Press, Cambridge, 184 (1978).

Lindt, J. T., "Note on the Wake Behind a Two-dimensional Bubble," *Chem. Eng. Sci.*, **26**, 1776 (1971).

Miyahara, T., Tsuchiya, K. and Fan, L.-S., "Wake Properties of a Single Bubble Accompanied by a Periodic Wake," *Int. J. Multiphase Flow*, **14**, 749 (1988).

Morooka, S., Uchida, K. and Kato, Y., "Recirculating Turbulent Flow of Liquid in Gas-liquid-solid Fluidized Bed," *J. Chem. Eng. Japan*, **15**, 29 (1982).

Muroyama, K., Fukuma, M. and Yasunishi, A., "Wall-to-bed Heat Transfer Coefficient in Gas-liquid-solid Fluidized Beds," *Can. J. chem. Engng.*, **62**, 199 (1984).

Nikov, I. and Delmas, H., Solid-liquid Mass Transfer in Three-phase Fixed and Fluidized Beds," *Chem. Eng. Sci.*, **42**, 1089 (1987).

Nguyen-Tien, Patwari, K., Schumpe, A. N. and Deckwer, W.-D., "Gas-liquid Mass Transfer in Fluidized Particle Beds," *AIChE Journal*, **31**, 194 (1985).

Nigam, K. D. P. and Schumpe, A., "Gas-liquid Mass Transfer in a Bubble Column with Suspended Solids," *AIChE Journal*, **33**, 328 (1987).

Østergaard, K., "Advances in Chemical Engineering," eds Drew, T. B., Cokelet, G. R., Hoopes, J. W. and Vermulen, T., Academic Press, New York (1968).

Østergaard, K. and Fosbø, P., "Transfer of Oxygen Across the Gas-liquid Interface in Gas-liquid Fluidized Bes," *Chem. Eng. J.*, **3**, 105 (1972).

Pandit, A. B. and Joshi, J. B., "Mass and Heat Transfer Characteristics of Three Phase Sparged Reactors," *Chem. Eng. Res. Des.*, **64**, 125 (1986).

Roy, N. K., Guha, D. K. and Rao, M. N., "Suspension of Solids in a Bubbling Liquid Critical Gas Flow Rates for Complete Suspension," *Chem. Engng. Sci.*, **19**, 215 (1964).

Saberian-Broudjenni, M., Wild, G., Midoux, N. and Charpentier, J. C., "Contribution a l'etude du transfert de chaleur a la paroi dans les reacteurs a lit fluidise gaz-liquide-solide a faible vitesse de liquide," *Can. J. chem. Engng.*, **63**, 553 (1985).

Sada, E., Kumazawa, H., Lee, C. H. and Narukawa, H., "Gas-Liquid Interfacial Area and Liquid-side Mass-transfer Coefficient in a Slurry Bubble Column," *Ind. Eng. Chem. Res.*, **26**, 112 (1987).

Sänger, P. and Deckwer, W.-D., "Liquid-solid Mass Transfer in Aerated Suspensions," *Chem. Engng. J.*, **22**, 179 (1981).

Schumpe, A., Saxena, A. K. and Fang, L. K., "Gas/Liquid Mass Transfer in a Slurry Bubble Column," *Chem. Engng. Sci.*, **42**, 1787 (1987).

Smith, D. N. and Ruether, J. A., "Dispersed Solid Dynamics in a Slurry Bubble Column," *Chem. Engng. Sci.*, **40**, 741 (1985).

Song, G.-H., Tsuchiya, K. and Fan, L.-S., "Image Processing Technique for Measurement of Solids Holdup in Near Wake Behind a Single Bubble in a Liquid-solid Fluidized Bed," *Chem. Eng. Sci.*, **46**, 2933 (1991).

Soung, W. Y., "Bed Expansion in Three-phase Fluidization," *Ind. Engng. Chem. Process Des. Dev.*, **17**, 33 (1978).

Suganuma, T. and Yamanishi, T., "Behavior of Solid Particles in Bubble Columns," *Kagaku Kogaku*, **30**, 1136 (1966).

Sun, Y., Nozawa, T. and Furusaki, S., "Gas Holdup and Volumetric Oxygen Transfer Coefficient in a Three-phase Fluidized Bed Bioreactor," *J. Chem. Eng. Japan*, **21**(1), 15 (1988).

Tsuchiya, K. and Fan, L.-S., "Near-wake Structure of a Single Gas Bubble in a Two-dimensional Liquid-solid Fluidized Bed: Vortex Shedding and Wake Size Variation," *Chem. Eng. Sci.*, **43**, 1167 (1988).

Tsutsumi, A., Kim, Y. H., Togawa, S. and Yoshida, K., "Classification of Three-phase Reactors," in Reactions & Reaction Engineering (Edited by Mashelkar, R. A. and Kumar, R.), Indian Academy of Sciences, Bangalore, 247 (1987).

Yasunishi, A., Fukuma, M. and Muroyama, K., "Hydrodynamics and Gas-liquid Mass Transfer Coefficient in a Slurry Bubble Column with High Solid Content," *Kagaku Kogaku Ronbunshu*, **12**, 420 (1986).